Investigation of weak interlayer exchange coupling in GaMnAs/GaAs superlattices with insulating nonmagnetic spacers

Jae-Ho Chung,[1] Young-Sang Song,[1] Taehee Yoo,[1] Sun Jae Chung,[1] Sanghoon Lee,[1,a)]
B. J. Kirby,[2] X. Liu,[3] and J. K. Furdyna[3]
[1]*Department of Physics, Korea University, Seoul, 136-701, Korea*
[2]*NIST Center for Neutron Research, Gaithersburg, Maryland 20899, USA*
[3]*Department of Physics, University of Notre Dame, Notre Dame, Indiana 46556, USA*

(Received 31 March 2011; accepted 6 June 2011; published online 11 July 2011)

A robust long-range antiferromagnetic coupling between ferromagnetic $Ga_{0.97}Mn_{0.03}As$ layers has previously been realized via insertion of nonmagnetic Be-doped GaAs spacers between the magnetic layers. In this paper we report the observation of weak antiferromagnetic coupling between $Ga_{0.97}Mn_{0.03}As$ layers through undoped GaAs spacers with thicknesses as large as 25 monolayers. The field and the temperature dependences of the sample magnetization suggest that the interlayer coupling in these systems substantially deviates from typical ferromagnetic behavior. Polarized neutron reflectivity measurements reveal antiferromagnetic alignment between $Ga_{0.97}Mn_{0.03}As$ layers when a weak field is applied perpendicular to the magnetic easy axis during cooling below T_C. The strength of the observed coupling between the magnetic layers is estimated to be weaker than 0.05 mT. © *2011 American Institute of Physics*. [doi:10.1063/1.3609080]

I. INTRODUCTION

The realization of antiferromagnetic (AFM) coupling between thin magnetic layers has important technological implications in the area of spintronics.[1] Its utility relies on the fact that charge carriers in the form of electrons or holes carry intrinsic magnetic moments, which in turn interact with magnetic moments within transport media. In this process, the resistance against the flow of spin-polarized charge carriers through ferromagnetic (FM) materials is influenced greatly by the relative orientation of the spin polarization with respect to the magnetization. This spin-dependent transport behavior has already found extensive applications in giant magnetoresistance (GMR) devices that are now in commercial use. Such GMR devices typically involve pairs of FM layers coupled via spontaneous AFM interlayer exchange coupling (IEC).[2–4] The relative magnetizations of the FM layers can then be easily manipulated by the external magnetic field, which often leads to large changes in electrical resistivity. One of the key elements for achieving the GMR effect is the ability to control the interlayer magnetic exchange coupling, either FM or AFM. In metallic ferromagnets this technology is based on the nature of the carrier-mediated Ruderman–Kittel–Kasuya–Yosida (RKKY) interaction, in which the exchange integral oscillates with alternating sign over the range of a few nanometers.[5,6] The AFM IEC is therefore typically observed across nonmagnetic spacers with thicknesses of less than a few nanometers in metallic multilayers.

In the case of semiconductor-based magnetic multilayers, the progress in controlling the IEC phenomenon has been rather slow, both in theory and in experiment. Earlier observations of AFM IEC in semiconducting ferromagnets were reported in rare-earth-based semiconductors, such as EuS/PbS or EuS/YbSe, in which the Curie temperatures (T_C) are as low as 18 K.[7,8] In structures involving diluted magnetic semiconductors (DMSs) such as GaMnAs, in which the T_C can reach as high as 170 K by the careful optimization of engineering parameters,[9–11] only the FM IEC has been observed for a long time.[12–16] Part of the reason for this may be that it is very difficult to adequately describe and predict the properties of these DMS systems in theoretical calculations. In principle, magnetic interactions in DMSs are expected to possess similar characteristics as in the metallic systems based on the RKKY mechanism.[17–22] Taking this into consideration, the IEC in GaMnAs-based multilayers has also been expected to exhibit oscillations between FM and AFM as a complicated function of the carrier density and/or distance between magnetic layers. It was only very recently, however, that a robust AFM coupling between GaMnAs layers has been realized in experiments.[23–26] This desirable coupling was achieved when Be was explicitly introduced into the nonmagnetic spacer layers as a p-type dopant (typically at the level of $p \approx 10^{20}/cm^3$).[23] Reversible switching between FM and AFM alignments was observed in both superlattice and trilayer configurations, which subsequently led to the realization of the GMR effect in electrical transport measurements in these systems.[25,26]

The previous works demonstrated the importance of sufficient carrier density in the spacer layers for realizing robust AFM IEC.[23,25] In those works magnetization, polarized neutron reflectivity, and magnetotransport measurements were used to confirm the presence of the AFM IEC in the samples with Be-doped spacers. The AFM IEC has, however, initially been predicted to occur in superlattice (SL) structures with no explicit carrier doping in the spacers.[19] This is because, even without extra doping, the charge density in the nonmagnetic spacers can be enhanced by spillover of the carriers

a)Electronic mail: slee3@korea.ac.kr.

from adjacent magnetic layers. Therefore, the AFM IEC can exist also in SL samples with no Be doping, however, the amplitude of its exchange oscillation is probably much weaker. The observation of the AFM IEC in SLs with periodicities as large as $d_{SL} \approx 50$ monolayers (ML) (and with nonmagnetic spacer thickness, $d_N \approx 25$ ML) is, however, still quite surprising,[25] because the available theories typically predict that the IEC should become negligible beyond 10 ML.[17–22] This suggests that the length scale of the IEC can be drastically different between metallic and DMS-based structures.

II. EXPERIMENTAL RESULTS

Among the several $Ga_{0.97}Mn_{0.03}As/GaAs$ SL samples previously investigated, in this paper we revisit the sample that contained no Be doping but showed behaviors suggesting a departure from normal FM IEC. This sample, which was labeled as A4 in Ref. 25, consists of 10 periods of alternating magnetic and non-magnetic layers with thicknesses of $d_M = 24.4$ ML and $d_N = 25.1$ ML, respectively, so that its total SL periodicity corresponds to $d_{SL} = 49.5$ ML. (The unit of the SL dimensions may be converted to nm by using the multiplication factor 3.54 ML/nm.) Note that in trilayer samples definitive FM IEC has been observed for undoped spacers up to $d_N = 21$ ML, but was rather inconclusive for 42-ML spacers.[16] The spacer thickness of our sample falls between these two values, but SL samples have not previously been investigated in detail up to this thickness.[13]

A. Magnetization measurements

Figure 1(a) summarizes the temperature dependence of the magnetization measured during cooling at a series of constant fields. The measurement was performed with the external field applied parallel to [110], which is the magnetic easy axis of the uniaxial anisotropy.[27] It is apparent that the magnetization of the A4 sample depends strongly on the strength of the external field. The magnetization at 50 mT is similar to the typical behavior of ferromagnetic GaMnAs. At lower fields, however, the magnetization is substantially suppressed relative to the saturation value, although not quite down to zero. In order to visualize how the magnetization depends on the field, the values of magnetization at different fields are extracted for each temperature from the data shown in Fig. 1(a), and are plotted in Fig. 1(b) as a function of the field. Note that the net direction of the magnetization of each layer is determined at $T \approx T_C$ where the anisotropy is very small,[27] and remains without reversal upon further cooling. The above presentation therefore avoids the locking of FM alignments due to the strong anisotropy that may occur during field sweeping, particularly at low temperatures. Figure 1(b) clearly shows that the magnetization curves experience a sharp downward turn at low fields below ~0.5 mT, which is particularly pronounced at low temperatures. Such field-dependent behavior indicates a departure from the typical FM IEC. Figures 1(c) and 1(d) show similar data obtained on sample A3, which was unambiguously shown to have FM IEC.[23,25] It is apparent that there is almost no field dependence in the magnetization of this sample, and especially that

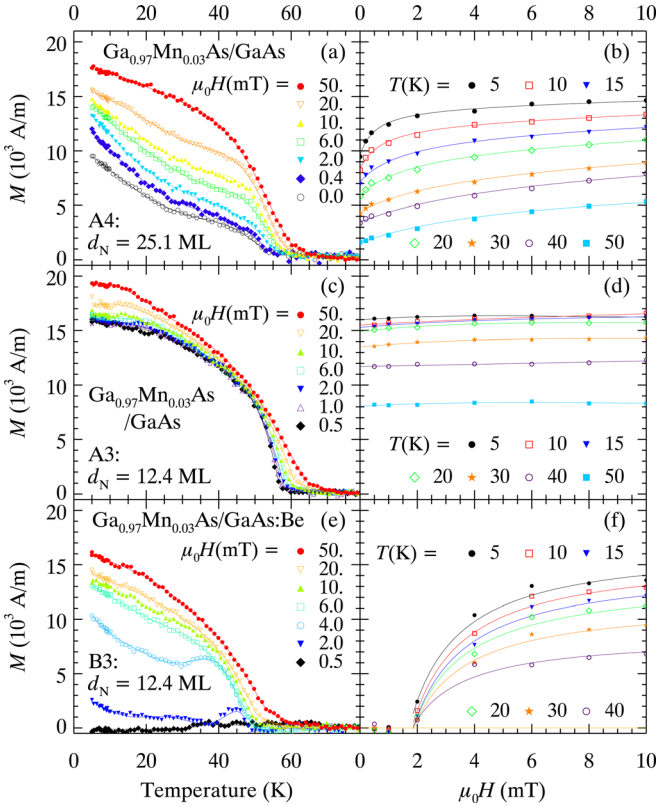

FIG. 1. (Color online) Magnetization measured during cooling under constant field applied along the [110] direction: (a) $Ga_{0.97}Mn_{0.03}As/GaAs$ (A4: $d_M = 24.4$ ML, $d_N = 25.1$ ML, and $d_{SL} = 49.5$ ML) (c) $Ga_{0.97}Mn_{0.03}As/GaAs$ (A3: $d_M = 24.4$ ML, $d_N = 12.4$ ML, and $d_{SL} = 36.8$ ML) and (e) $Ga_{0.97}Mn_{0.03}As/GaAs$:Be (B3: $d_M = 24.4$ ML, $d_N = 12.4$ ML, and $d_{SL} = 36.8$ ML). The right panels show the field dependence of the magnetization obtained by interpolating the magnetization data shown in the left. The lines are guides to the eye.

the downward dip is absent. On the contrary, we find that the behavior of sample A4 is rather similar to that of B3 (which was shown to have robust AFM IEC in earlier experiments),[23,25] as seen in the data in Figs. 1(e) and 1(f). Both samples reveal sharp decreases of magnetization at fields below 4 mT, which are ascribed to cancellations of net magnetization due to the AFM IEC. These data suggest that the low-field behavior of sample A4 reveals similarities to the behavior of B3, thus suggesting the likelihood of AFM IEC in that sample.

The presence of AFM IEC in sample A4 is also suggested in the M versus H data. The M - H (‖ [110]) hysteresis curves at selected temperatures are plotted in Fig. 2. The data at 10 K show a nearly square-shaped hysteresis loop similar to typical FM behavior. The initial magnetization curve, plotted as a solid line in Fig. 2(a), however, is clearly distinguished from the main loop. It indicates that the net magnetization after zero-field cooling is significantly smaller compared to remnant magnetization after field cycling, suggesting that the associated magnetic layers are not altogether aligned parallel to each other. We note that these SL samples tend to form a single domain even over a fairly large area,[13] unless intentionally broken up by precisely controlling the external field.[28] Therefore the observed behavior is not likely to be due to domain formation. As the temperature increases, the hysteresis loops become more rounded, and both the

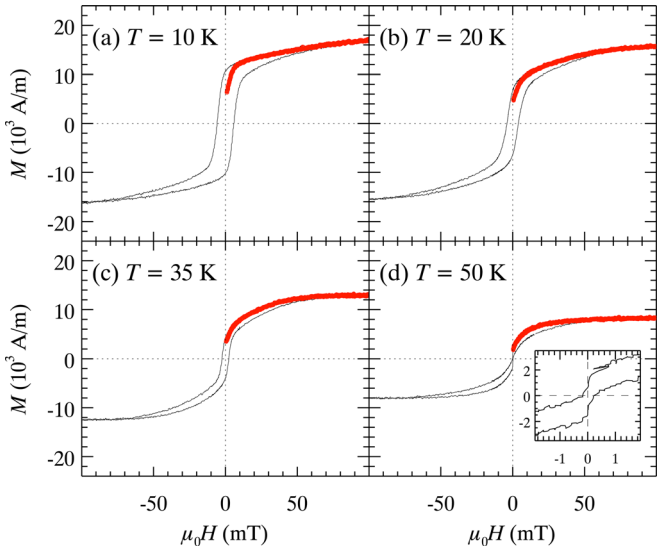

FIG. 2. (Color online) M vs $\mu_0 H$ hysteresis loops of the A4 ($Ga_{0.97}Mn_{0.03}As$/GaAs, $d_M = 24.4$ ML, $d_N = 25.1$ ML, and $d_{SL} = 49.5$ ML) SL sample. The thick red lines indicate the initial magnetization after zero-field cooling. The inset in (d) shows the hysteresis loop near zero field.

remnant magnetization and the coercive field are reduced, owing to the reduction of the cubic anisotropy. Above 30 K, where the cubic anisotropy becomes weaker than the uniaxial anisotropy,[27] the magnetization shows a sharp downturn near zero field. This behavior is consistent with the AFM coupling between the layers overcoming the weak magnetic anisotropy.

In Fig. 3(b) we plot the remnant magnetization (at $\mu_0 H = 0$ mT; open squares) and the saturation magnetization (at $\mu_0 H = 100$ mT; closed circles) measured for sample A4. These plots show that the remnant magnetization is substantially reduced in comparison to the saturation magnetization throughout the temperature range below T_C. The remnant and saturation magnetization data for two other SL samples, A3 and B3, are also plotted for comparison in Figs. 3(a) and 3(c), respectively. These two latter samples have the same dimensions ($d_M = 24.4$ ML, $d_N = 12.4$ ML, and $d_{SL} = 36.8$ ML), however only B3 has the nonmagnetic spacers doped with Be. Consequently, B3 exhibits a robust AFM IEC, whereas A3 has a typical FM IEC.[23,25] When all three samples are compared, the behavior of A4 is seen to be closer to that of B3 than A3. It is also important to point out that the rates of change in the remnant magnetization in both A4 and B3 are clearly larger below 20 K than above 20 K. In contrast, the A3 sample with FM IEC shows no significant temperature dependence.

Compared to the AFM IEC in sample B3 that was previously reported, the IEC of sample A4 appears to be much weaker, i.e., the magnetization of the A4 is not fully canceled even in zero field. One reason for this can be that the AFM IEC may not cover the entire area of the SL sample that consists of 10 periods of magnetic/nonmagnetic layers due to possible fluctuations in the layer thickness. This may also be partially due to a weak remnant field of the magnetometer, which can cause accidental ferromagnetic alignment when the spontaneous AFM coupling is weak. For this reason, the apparent observation of FM alignments may not necessarily be an indication of FM IEC.

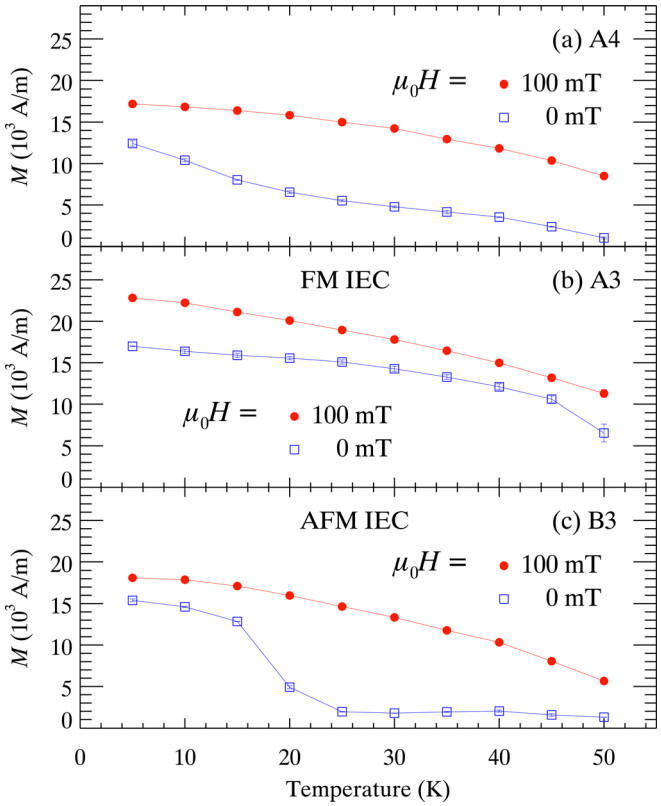

FIG. 3. (Color online) The temperature dependence of the saturation magnetization ($\mu_0 H = 100$ mT; closed circles) and the remnant magnetization ($\mu_0 H = 0$ mT; open squares) for (a) A4, (b) A3, and (c) B3.

B. Polarized neutron reflectivity measurements

Polarized neutron reflectivity was used in our previous work to confirm the presence of AFM IEC in the Be-doped SL samples,[23–25] but this method can also be affected by the presence of a weak remnant field during the cooling process. In order to minimize this unwanted effect, we intentionally exposed sample A4 to a remnant field along two different directions while the sample was cooled down below its T_C. Figure 4 schematically shows the experimental configurations, in which the angle between the guide field and the

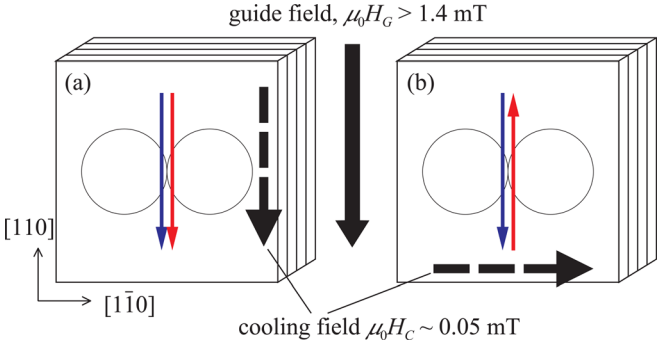

FIG. 4. (Color online) Description of the directions of the cooling field (dashed arrows, $\mu_0 H_C$), guide field (solid arrow, $\mu_0 H_G$), and the lattice orientations in the polarized neutron reflectivity measurements. The double-ended circles represent constant-energy surfaces of the uniaxial anisotropy. The thin arrows indicate either (a) FM, or (b) AFM spin arrangements between magnetic layers.

cooling field is varied. The guide field (H_G), which is necessary in order to maintain neutron polarization, is fixed along the [110] direction during the reflectivity measurements. During the cooling process, the guide field was turned off, and the direction of the cooling field (H_C) was varied to be either parallel [see Fig. 4(a)] or perpendicular [see Fig. 4(b)] to the [110] direction by rotating the sample. Note that during the initial cooling process ($T_C/2 < T < T_C$) the weak uniaxial anisotropy is present and the magnetic easy axis is parallel to the [110] direction.[27] Therefore, the cooling field parallel to the easy axis can break the initial weak AFM IEC, resulting in the FM alignment of the magnetic layers. In contrast, the AFM IEC and the corresponding alignment can be less affected if the cooling field is applied perpendicular to the easy axis. Once cooled down below $T \approx T_C/2$, the magnetization vectors will be locked due to the onset of strong cubic anisotropy unless exposed to a sufficiently strong external field.

The polarized neutron reflectivity measurements were performed using the NG1 reflectometer at the NIST Center for Neutron Research. The details of the experimental setup are discussed in an earlier work.[23] The strength of the field during the cooling process was approximately $H_C \approx 0.05$ mT, whereas the guide field was varied at $H_G = 1.4$ mT or higher. The data collected at 6 K in two configurations (see Fig. 4) are summarized and compared in Fig. 5. It is important to stress that the splitting between the two non-spin-flip (NSF) channels, (++) and (− −), occurs due to the magnetization components of the SL sample that are parallel to the guide field.[29] The data measured after cooling with $H_C \parallel [110]$ show the splitting at the wave vector equivalent to the SL period, $Q_{FM} = Q_{SL} = 2\pi/(d_M + d_N) = 0.045$ Å^{-1}. Full dynamical calculations confirm that this feature is indicative of equivalent magnetic and structural periodicity—indicating FM alignment.[30,31] The solid lines in Fig. 5 are the model calculations using the simple FM (or AFM) alignment between adjacent magnetic layers.[32]

In contrast, when the data were measured after cooling with $H_C{}^{\perp}[110]$, the splitting is observed at the wave vector, $Q_{\mathrm{AFM}} = Q_{\mathrm{SL}}/2 = \pi/(d_{\mathrm{M}} + d_{\mathrm{N}}) = 0.023$ Å^{-1}, which corresponds to twice o the SL period. This means that the alignment of the magnetization is antiparallel between adjacent magnetic layers, i.e., that the IEC is AFM [see Fig. 5(b).] This AFM alignment, however, is destroyed when the magnetic field is increased beyond the anisotropy field (see the $H_G = 30$ mT data in Fig. 5). As a result, the splitting between the two NSF channels moves back to Q_{FM}, indicating the field-induced formation of the FM alignment. The above process was repeated several times to ensure that the splitting reproducibly occurs for each configuration. These results indicate that the strength of the AFM IEC near T_C is weak enough to be easily overcome by a field of 0.05 mT. Lower values of H_C or H_G were not practically achievable at our experimental setup. Although not shown, additional measurements with H_C ($\parallel [110]$) ≥ 0.05 mT were all consistent with FM alignments.

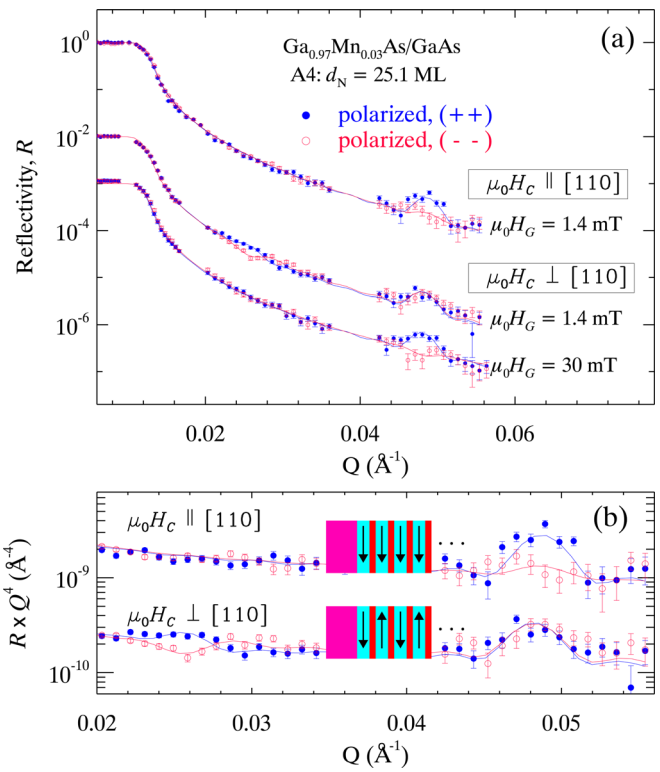

FIG. 5. (Color online) Polarized neutron reflectivity of the GaMnAs/GaAs (A4) SL sample measured at 6 K. The data are vertically shifted for clarity. H_C and H_G denote the cooling field and the guide field, respectively. Solid lines are the full dynamical calculations using the REFLPAK program (see Ref. 32) for SL magnetization alignments as illustrated in the middle of (b). In panel (b), only the data measured at $\mu_0 H_G$ ($\parallel [110]$) = 1.4 mT are shown.

III. DISCUSSION

Until now, many research groups have attempted theoretical calculations for the IEC and/or its oscillations expected from the RKKY theory.[17–22] In these works, the length scale of the IEC was discussed either in terms of the SL period[17,21,22] or the spacer thickness.[19,33] The former is probably more appropriate for SL structures, whereas the latter is more appropriate for trilayers. The existing theoretical calculations, however, may not be directly compared to the experimental results using SL samples, because these earlier calculations usually did not consider situations involving large layer thicknesses. In contrast, experiments on SL samples often use magnetic layers thicker than 10 ML.[13,15,23,25] In some cases it was even predicted that SL samples with thick magnetic layers will not produce AFM IEC,[21] which clearly contradicts experimental observations. Therefore, we argue that all three parameters, d_{M}, d_{N}, and d_{SL}, should be rigorously included in theoretical calculations.

Our experimental results suggest two potentially important ideas regarding IEC in GaMnAs/GaAs-based SL samples with large layer thicknesses, which have not been explicitly taken into account in the existing theories. First, the experimental results suggest that the exchange oscillations expected from the RKKY theory have much larger length scales than previously expected. Previously, in all the other SL samples with thinner spacers without Be doping we observed only FM IEC.[25] Therefore, the change of sign of the IEC from FM to AFM should occur at the SL period

between d_{SL} ~37 ML and ~50 ML (or d_N ~12.5 ML and ~25 ML). In contrast, the change of sign of the IEC in the case of Be-doped spacers was observed for the SL periods between 32.6 ML and 36.8 ML (or $d_N = 8.1$ ML and 12.4 ML).[25] Since the AFM IEC has never been observed for SL samples with shorter periods, these must correspond to sign changes occurring at the shortest period for the specific Be concentrations. A similar result has been reported in the case of trilayers, in which the AFM IEC was observed for a Be-doped spacer with $d_N = 15$ ML.[26] All of these data consistently provide evidence that the IEC in GaMnAs/GaAs systems is long-ranged compared to theoretical predictions. The apparent contradiction may be due to the difficulty of considering extended dimensions in theoretical calculations. Furthermore, a direct comparison between the two series (Be-doped and undoped) suggests that both the oscillation amplitude and the period depend strongly on the carrier density in the SL. The present results particularly suggest that the length scale of IEC, or its oscillation period, is more long-ranged when the carrier density is lower. Therefore, it appears beneficial to have higher carrier concentrations in the nonmagnetic spacers in order to achieve AFM IEC.

IV. CONCLUSIONS

In summary, we have used magnetization measurements and polarized neutron reflectivity to investigate the nature of exchange coupling between magnetic layers in a $Ga_{0.97}Mn_{0.03}As$/GaAs SL with $d_{SL} = 49.5$ ML, which was labeled as A4 in earlier work.[25] Although the coupling between the magnetic layers is very weak in this sample, the antiparallel spin alignment between the magnetic layers reproducibly appeared when a weak cooling field was applied perpendicular to the magnetic easy axis. Magnetization measurements also suggest that AFM IEC exists, at least partially, in this sample. These results indicate that the dimension of the investigated sample is in the proximity of the oscillation boundary where the exchange coupling changes sign. This is consistent with the picture of long-range IEC observed recently in a related series of samples with Be doping in the nonmagnetic spacer layers.

ACKNOWLEDGMENTS

We are grateful to Julie Borchers for technical support during polarized neutron reflectivity measurements and helpful discussions. This work is supported by the Mid-Career Research Program (Grant Nos. 2010-0025880 and 2009-0085028), and the Nuclear R&D Program (Grnat No. 2010-0018369) through the NSF grant funded by the Ministry of Education, Science, and Technology. The work at Notre Dame was supported by the National Science Foundation Grant No. DMR 10-05851.

[1] P. Grünberg, R. Schreiber, Y. Pang, M. B. Brodsky, and H. Sowers, Phys. Rev. Lett. **57**, 2442 (1986).
[2] M. N. Baibich, J. M. Broto, A. Fert, F. N. Vandau, F. Petroff, P. Eitenne, G. Creuzet, A. Friederich, and J. Chazelas, Phys. Rev. Lett. **61**, 2472 (1988).
[3] J. Barnaś, A. Fuss, R. E. Camley, P. Grünberg, and W. Zinn, Phys. Rev. B **42**, 8110 (1990).
[4] P. Grünberg, S. Demokritov, A. Fuss, M. Vohl, and J. A. Wolf, J. Appl. Phys. **69**, 4789 (1991).
[5] S. S. P. Parkin, N. More, and K. P. Roche, Phys. Rev. Lett. **64**, 2304 (1990).
[6] P. Bruno, Phys. Rev. B **52**, 411 (1995).
[7] C. J. P. Smits, A. T. Filip, H. J. M. Swagten, B. Koopmans, W. J. M. de Jonge, M. Chernyshova, L. Kowalczyk, K. Grasza, A. Szczerbakow, T. Story, W. Palosz, and A. Y. Sipatov, Phys. Rev. B **69**, 224410 (2004).
[8] H. Kępa, C. Majkrzak, A. Sipatov, and T. Giebultowicz, Physica B **397**, 36 (2007).
[9] K. C. Ku, S. J. Potashnik, R. F. Wang, S. H. Chun, P. Schiffer, N. Samarth, M. J. Seong, A. Mascarenhas, E. Johnston-Halperin, R. C. Myers, A. C. Gossard, and D. D. Awschalom, Appl. Phys. Lett. **82**, 2302 (2003).
[10] A. M. Nazmul, S. Sugahara, and M. Tanaka, Phys. Rev. B **67**, 241308(R) (2003).
[11] A. H. MacDonald, P. Schiffer, and N. Samarth, Nature Mater. **4**, 195 (2005).
[12] T. Dietl, J. Cibert, D. Ferrand, and Y. M. d'Aubigne, Mater. Sci. Eng., B **63**, 103 (1999).
[13] H. Kępa, J. Kutner-Pielaszek, A. Twardowski, C. F. Majkrzak, J. Sadowski, T. Story, and T. M. Giebultowicz, Phys. Rev. B **64**, 121302(R) (2001).
[14] R. Mathieu, P. Svedlindh, J. Sadowski, K. Światek, M. Karlsteen, J. Kanski, and L. Ilver, Appl. Phys. Lett. **81**, 3013 (2002).
[15] S. J. Chung, S. Lee, I. W. Park, X. Liu, and J. K. Furdyna, J. Appl. Phys. **95**, 7402 (2004).
[16] B. J. Kirby, J. A. Borchers, X. Liu, Z. Ge, Y. J. Cho, M. Dobrowolska, and J. K. Furdyna, Phys. Rev. B **76**, 205316 (2007).
[17] T. Jungwirth, W. A. Atkinson, B. H. Lee, and A. H. MacDonald, Phys. Rev. B **59**, 9818 (1999).
[18] J. S. Hong, D. S. Wang, and R. Q. Wu, Phys. Rev. Lett. **94**, 137206 (2005).
[19] P. Sankowski and P. Kacman, Phys. Rev. B **71**, 201303(R) (2005).
[20] T. Jungwirth, J. Mašek, J. Kučera, and A. H. MacDonald, Rev. Mod. Phys. **78**, 809 (2006).
[21] A. D. Giddings, T. Jungwirth, and B. L. Gallagher, Phys. Status Solidi C **3**, 4070 (2006).
[22] A. D. Giddings, T. Jungwirth, and B. L. Gallagher, Phys. Rev. B **78**, 165312 (2008).
[23] J.-H. Chung, S. J. Chung, S. Lee, B. J. Kirby, J. A. Borchers, Y. J. Cho, X. Liu, and J. K. Furdyna, Phys. Rev. Lett. **101**, 237202 (2008).
[24] S. Lee, J. H. Chung, X. Y. Liu, J. K. Furdyna, and B. J. Kirby, Mater. Today **12**, 14 (2009).
[25] S. Chung, S. Lee, J. H. Chung, T. Yoo, H. Lee, B. Kirby, X. Liu, and J. K. Furdyna, Phys. Rev. B **82**, 054420 (2010).
[26] J. Leiner, H. Lee, T. Yoo, S. Lee, B. J. Kirby, K. Tivakornsasithorn, X. Liu, J. K. Furdyna, and M. Dobrowolska, Phys. Rev. B **82**, 195205 (2010).
[27] D. Y. Shin, S. J. Chung, S. Lee, X. Liu, and J. K. Furdyna, Phys. Rev. B **76**, 035327 (2007).
[28] D. Y. Shin, S. J. Chung, S. Lee, X. Liu, and J. K. Furdyna, Phys. Rev. Lett. **98**, 047201 (2007).
[29] C. F. Majkrzak, Physica B **173**, 75 (1991).
[30] C. F. Majkrzak, Physica B **221**, 342 (1996).
[31] C. F. Majkrzak, K. V. O'Donovan, and N. F. Berk, in *Neutron Scattering from Magnetic Materials*, edited by T. Chatterji (Elsevier, New York, 2005).
[32] P. A. Kienzle, K. V. O'Donovan, J. F. Ankner, and N. F. Berk, REFLPAK, http://www.ncnr.nist.gov/reflpak (2000–2006).
[33] K. Szałowski and T. Balcerzak, Phys. Rev. B **79**, 214430 (2009).